Molecular Neurobiology (2024) 61:4146–4165
https://doi.org/10.1007/s12035-023-03825-7

Oligodeoxynucleotide IMT504: Effects on Central Nervous System Repair Following Demyelination

Patricia A. Mathieu[1,2] · Yim Rodriguez Sampertegui[1,2] · Fernanda Elias[3] · Alexis Silva Silva[1,2] · María de Luján Calcagno[4] · Ricardo López[5] · Ana M. Adamo[1,2]

Received: 29 May 2023 / Accepted: 21 November 2023 / Published online: 8 December 2023

Abstract

Multiple sclerosis (MS) is an immune-mediated central nervous system (CNS) disease characterized by demyelination resulting from oligodendrocyte loss and inflammation. Cuprizone (CPZ) administration experimentally replicates MS pattern-III lesions, generating an inflammatory response through microgliosis and astrogliosis. Potentially remyelinating agents include oligodeoxynucleotides (ODN) with a specific immunomodulatory sequence consisting of the active motif PyNTTTTGT. In this work, the remyelinating effects of ODN IMT504 were evaluated through immunohistochemistry and qPCR analyses in a rat CPZ-induced demyelination model. Subcutaneous IMT504 administration exacerbated the pro-inflammatory response to demyelination and accelerated the transition to an anti-inflammatory state. IMT504 reduced microgliosis in general and the number of phagocytic microglia in particular and expanded the population of oligodendroglial progenitor cells (OPCs), later reflected in an increase in mature oligodendrocytes. The intracranial injection of IMT504 and intravenous inoculation of IMT504-treated B lymphocytes rendered comparable results. Altogether, these findings unveil potentially beneficial properties of IMT504 in the regulation of neuroinflammation and oligodendrogenesis, which may aid the development of therapies for demyelinating diseases such as MS.

Keywords Cuprizone · Demyelination · Remyelination · Oligodeoxynucleotide IMT504

Abbreviations

ANOVA	Analysis of variance
Arg1	Arginase 1
BSA	Bovine serum albumin
CC	Corpus callosum
CD24	Cluster of differentiation 24
CD38	Cluster of differentiation 38
CD59	Cluster of differentiation 59
CD68	Cluster of differentiation 68
CICUAL	Comité Institucional para el Cuidado y Uso de Animales de Laboratorio
CIOMS	Council for International Organizations for Medical Science
CNS	Central nervous system
CpG	Unmethylated cytosine-guanosine dinucleotides
CPZ	Cuprizone
Ct	Cycle threshold
GAPDH	Glyceraldehyde-3-phosphate dehydrogenase
IFNα	Interferon alpha
Iba1	Ionized calcium-binding adaptor molecule 1
ICLAS	International Council for Laboratory Animal Science
IL-1β	Interleukin-1β
IL 10	Interleukin 10
IL 35	Interleukin 35
IHC	Immunohistochemistry
iNOS	Inducible nitric oxide synthase

✉ Ana M. Adamo
anadamo@ffyb.uba.ar; anamadamo@gmail.com

1 Facultad de Farmacia y Bioquímica, Departamento de Química Biológica, Universidad de Buenos Aires, Junín 956, C1113AAD Buenos Aires, Argentina

2 CONICET, Instituto de Química y Fisicoquímica Biológicas (IQUIFIB), Universidad de Buenos Aires Junín 956, C1113AAD Buenos Aires, Argentina

3 Instituto de Ciencia y Tecnología Dr. César Milstein (CONICET-Fundación Pablo Cassará), Saladillo 2468, C1440FFX Buenos Aires, Argentina

4 Facultad de Farmacia y Bioquímica, Departamento de Fisicomatemática, Universidad de Buenos Aires, Junín 956, C1113AAD Buenos Aires, Argentina

5 Immunotech S.A., Buenos Aires, Argentina

IC	Intracranial injection
IV	Injected into the tail vein
LB	Lymphocyte B
MAG	Myelin-associated glycoprotein
MBP	Myelin basic protein
MHC I	Major histocompatibility complex I
MHC II	Major histocompatibility complex II
mRNA	Messenger ribonucleic acid
MS	Multiple sclerosis
NG2	Neural/glial antigen 2
NSC	Neural stem cell
ODN	Oligodeoxynucleotide
OL	Oligodendrocyte
OPC	Oligodendrocyte precursor cell
PBS	Phosphate-buffered saline
PBST	PBS containing 0.1% Triton
PDGFRα	Platelet-derived growth factor receptor alpha
qPCR	Quantitative polymerase chain reaction
RNA	Ribonucleic acid
RRID	Research Resource Identifiers
SC	Via subcutaneous
SEM	Standard error of the mean
SNPs	Single-nucleotide polymorphisms
SS	Saline solution
SVZ	Subventricular zone
TGF-β	Transforming growth factor beta
Wnt	Blending of the name of the Drosophila segment polarity gene Wingless and the name of the vertebrate homolog, integrated or int-1

Introduction

Characterized by focal white matter demyelination and inflammation, multiple sclerosis (MS) constitutes the most frequent immune-mediated disorder of the central nervous system (CNS) [1–4]. While demyelination is the pathological loss of myelin sheaths from around axons, remyelination is the process of myelin sheath restoration and axonal functional recovery [5, 6]. In the CNS, demyelination usually results from a direct insult on oligodendrocytes (OLs), while remyelination is spearheaded by NG2-expressing oligodendroglial progenitor cells (OPCs). However, different human and animal studies have recently demonstrated that mature OLs that survive in the demyelinated area have the capacity to regenerate myelin [7]. Although some nuclear receptors have been shown to contribute to myelin repair, frequently unsuccessful remyelination in MS seems to respond to a wide range of lesion-associated factors which hinder OPC maturation, including myelin debris, semaphorins, extracellular matrix molecules, sulfate proteoglycans, Wnt, LINGO-1, bone morphogenetic protein (BMP) [8, 9], and Notch signaling [10].

Among neural cells, OPCs account for the largest proliferating cell population and are uniformly distributed throughout the CNS [11]. OPCs can become OLs during CNS development or else remain quiescent and undifferentiated along adulthood until CNS injury triggers their proliferation and differentiation [12]. In the context of certain pathological scenarios during adulthood, neural stem cells (NSCs) residing in the subventricular zone (SVZ) can also become OPCs which then migrate into the corpus callosum (CC), striatum, or fimbria fornix, and mature into myelinating OLs [13–15]. The role of microglia should also be highlighted in the control of homeostasis and in the response to infection or damage in the CNS. Microglial activation occurs in different neurological disorders and could have a positive or negative effect, although a regenerative function has been attributed to microglia after demyelination [16]. Microglia can have a promyelinating effect after CNS myelin injury through the clearance of myelin debris, the secretion of specific cytokines and growth factors, and the modulation of the extracellular matrix [17].

Cuprizone (bis-cyclohexanone oxalydihydrazone, CPZ) administration is regarded as a useful model to replicate pattern-III lesions [18] characteristic of progressive forms of MS. Our group pioneered the histological and biochemical characterization of CPZ-induced demyelination in rats [19] and produced evidence of Notch and TGF-β involvement in cell fate decisions of adult brain SVZ NSC cultures and their implications in OPC proliferation and maturation [20]. We further characterized the inflammatory response showing both microgliosis and astrogliosis and reported cell-type- and ligand-specific Notch activation and its time- and area-dependent involvement in demyelination and spontaneous remyelination [21].

Innate receptors such as Toll-like receptors (TLRs) are implicated in the pathogenesis of CNS inflammatory disorders, including MS, and in experimental autoimmune encephalomyelitis (EAE), one of the animal models of demyelination. Unmethylated cytosine-phosphate-guanosine (CpG)-rich oligodeoxynucleotides (ODNs), typically found in microbial genomes, are potent activators of TLR9 in plasmacytoid dendritic cells (pDCs) and B cells. Dieu et al. have shown that intrathecal treatment with CpG induces the activation of type I interferon (IFN) signaling through an increase in IFNβ and suppresses EAE [22]. On the other hand, some results suggest a pro-inflammatory role for TLR9 in EAE [23], while other studies show that TLR9 deficiency exacerbates EAE, thus hinting at an immunoregulatory role [24].

Regarding the search for agents which may foster therapeutic strategies, a novel class of synthetic non-CpG ODNs features a specific immunomodulatory sequence consisting of the active motif PyNTTTTGT (Py, C or T; N, A or C or G or T) linked to a nuclease-resistant phosphorothioate

backbone. IMT504, the prototype of the immunostimulatory ODN of the PyNTTTTGT class, is 24-base long, with phosphorotioate bonds and the following nucleotide sequence: (5') TCATCATTTTGTCATTTTGTCATT (3'). It has been demonstrated that IMT504 directly activates lymphocytes B (LBs) and pDCs and is thus an excellent vaccine adjuvant [25, 26]. Moreover, IMT504 is a potent stimulator of mesenchymal stem cell expansion both in vitro and in vivo, which hints at beneficial applications for tissue repair therapies [27]. IMT504 has also proven effective in ameliorating chronic lymphocytic leukemia [28], neuropathic pain [29–31], and sepsis [32].

Most importantly, recent studies have shown that IMT504 stimulates human B regulatory cells by increasing the expression of Mucin 1, CD59, CD24, and CD38 and the secretion of interleukin (IL)-10 and IL-35 (Elías, *et al*., 2021, unpublished data). These results strongly suggest a role for IMT504 in many inflammatory and/or autoimmune disorders including arthritis, type 1 diabetes, psoriasis, asthma, MS, Alzheimer's and Parkinson's disease, all of which lack efficient treatment. Preclinical studies in turn indicate an excellent safety profile [33, 34]. In addition, OLs have the capacity to express immunomodulatory molecules such as cytokines and chemokines, antigen-presenting molecules and complement regulatory molecules such as CD59, a complement membrane attack inhibitor [35, 36]. For these reasons, IMT504 may be thought to have promyelinating effects either by modulating microglial polarization or fostering OPC proliferation and differentiation.

On the basis of these previous findings, the aim of the present work was to establish the possible remyelinating effects of IMT504 in a rat CPZ-induced demyelination model. To this end, experiments were conducted in vivo using subcutaneous (SC) or intracranial (IC) injections of IMT504 and intravenous (IV) injections of IMT504-treated LBs, as well as in vitro using primary microglia and OPC cultures.

Materials and Methods

Materials

CPZ (bis-cyclohexanone oxalhydrozone; cat #C9012), bovine serum albumin (BSA), paraformaldehyde (cat #158127), Hoechst 33258 (cat #B2883), and Triton X-100 (cat #T9284) were purchased from Sigma Chemical Co. (St. Louis, MO, USA). IMT504 was kindly provided by Fundación Pablo Cassará (ICT Milstein-CONICET, Buenos Aires, Argentina). DMEM/F12 culture medium and B27 were purchased from Gibco-ThermoFisher (Grand Island, NY, USA). Fetal bovine serum (FBS) was purchased from NATOCOR (Córdoba, Argentina). FGF-2 and PDGF-AA were purchased from PreproTech (Rocky Hill, NJ, USA). Primary and secondary antibodies are listed in Supplementary Tables 1 and 2. All other chemicals were analytical grade reagents of the highest purity available.

Animals

An in-bred strain of Wistar rats (RRID: RGD_13508588) was initially obtained from the animal facility of Facultad de Farmacia y Bioquímica and raised in our own animal room. All procedures were compliant with the Guide for the Care and Use of Laboratory Animals, National Research Council (US) Committee for the Update of the Guide for the Care and Use of Laboratory Animals, 8th edition (2011) and the International Guiding Principles for Biomedical Research Involving Animals, CIOMS and ICLAS (2012). The experimental protocol was approved before implementation by the Institutional Committee for the Care and Use of Laboratory Animals (Comité Institucional para el Cuidado y Uso de Animales de Laboratorio, CICUAL) at Facultad de Farmacia y Bioquímica, Universidad de Buenos Aires. Animals of either sex were housed at a maximum of 3 animals of the same sex per cage under controlled temperature (22° ± 2 °C), fed water and food ad libitum, and kept in a cycle of 12-h light/dark. The total number of animals used and evaluated was 184 and no animals were excluded. Three to five rats of either sex were used for all experiments. No randomization was performed to allocate subjects in the study. No sample calculation was performed but sample conventions from the field were used [19, 21, 37]. The immunohistochemistry (IHC) and immunocytochemistry (ICC) experiments were performed by experimenters who were blinded to the experimental design. All tests were conducted between 9 am and 5 pm.

Assessment of TLR9 Activation by CpG ODN 2006 and Non-CpG ODN IMT504

To assess whether IMT504 acts through TLR9, assays were conducted on human embryonic kidney HEK 293 cells which stably express human TLR9 (HEK 293-hTLR9) (kindly donated by Dr. M. D. Klinman). Cells were cultured in Dulbecco's modified Eagle medium (DMEM; Gibco, Scotland, UK) supplemented with 10% (v/v) FBS in the presence of 10 µg/ml Blasticidin S HCL (Invivogen, ant-bl-05) and 5% CO_2 in 96-well flat bottom plates (1–2 × 10^4 cells/well). Once 90–95% confluence was reached, cells were transfected with Lipofectamine 2000 (Gibco, cat. 18324012) and the following plasmids: pGL2 NF-kB Luc (0.04 µg) and pCMV Sport ß-galactosidase (0.12 µg) for assay standardization. After 24 h in culture, cells were stimulated with IMT504 and CpG ODN 2006 as a positive control, at a concentration of 15 µg/ml (2 µM) and incubated in culture medium (negative control). After 24 h, the culture

medium was removed, cells were lysed, and luciferase activity was determined using a commercial kit (Luciferase Assay System E 1500, Promega, Fitchburg, WI, USA). For the luciferase assay, samples were read in a luminometer (Luminometer Hidex 425-014, Turku, Finland) for 1 min. Samples were kept in the dark and at room temperature throughout the procedure.

Toxic CPZ-Induced Demyelination Protocol and IMT504 Treatment by Subcutaneous (SC) Injection

Twenty-one-day-old rats were housed at a maximum of 3 same-sex animals per cage in a temperature- (22° ± 2 °C) and photoperiod- (12-h light/dark) controlled room and fed chow without (control) or with 0.6% (w/w) CPZ (CPZ) ad libitum for 14 days. The protocol used in the current study, i.e., CPZ dose, anesthetics, treatment duration, animal sex distribution, and housing conditions, was selected on the basis of previous work by our group and others [19, 21, 38, 39].

In addition, a subset of both control and CPZ animals received 20 mg/kg body weight IMT504 [34] (control-IMT504 and CPZ-IMT504, respectively) or sterile saline solution (control-SS and CPZ-SS, respectively) via SC injection once a day over 5 days before CPZ withdrawal from the diet. Animals were then returned to a control diet and sacrificed upon CPZ withdrawal and last IMT504 injection (T0), 3 days (T3), 7 days (T7), 10 days (T10), 12 days (T12), or 21 days (T21) after CPZ withdrawal and last IMT504 injection. At the end of treatment periods, between 3 and 5 animals per group, per time point, were either deeply anesthetized with a ketamine/xylazine cocktail (75 mg and 10 mg per kg of body weight, respectively, according to the protocol approved by the CICUAL) and their brains excised and processed for IHC and electron microscopy analysis, or killed by decapitation and their corpus callosum (CC) dissected and frozen at − 80 °C for real-time polymerase chain reaction (qPCR) analyses.

Toxic CPZ-Induced Demyelination and IMT504 Treatment by Intracranial (IC) Injection in the CC

CPZ-demyelinated rats were IC injected with SS in the contralateral hemisphere or IMT504 in the ipsilateral hemisphere upon CPZ withdrawal. Rats were deeply anesthetized with a ketamine/xylazine cocktail (75 mg and 10 mg per kg of body weight, respectively), positioned in a stereotaxic frame and injected 20 µg of IMT504 in 1 µl of sterile SS. The ODN or the SS was injected into the CC (ipsilateral or contralateral, respectively) using the stereotaxic coordinates 0.5 mm anterior relative to bregma, 1.5 mm mediolateral, and 2.5 mm dorsoventral from the surface of the skull, and the needle was kept in place for 5 min to reduce reflux along the needle track. Animals were then returned to a control diet and 3 animals per group per time point, sacrificed at 3, 7, and 10 days (T3, T7, and T10, respectively) after the IC injection of IMT504 or SS. Brains were excised and processed for IHC.

Toxic CPZ-Induced Demyelination and IMT504-Treated LB Inoculation Through Intravenous (IV) Injection

Isolation and Culture of LBs

Spleens were isolated from naive 8–10-week-old female Wistar rats. Cells were obtained under aseptic conditions. Briefly, the organs were mashed through a 70-µm cell strainer (BD Biosciences, Franklin Lakes, NJ, USA) in RPMI medium supplemented with 10% FBS. LBs were purified by negative selection with EasySep Rat B Cell Isolation Kit (StemCell Technologies, Vancouver, Canada). Cell purity (≈ 98%) was evaluated by flow cytometry using a mouse anti-rat CD45RA antibody conjugated to R. Phycoerythrin (RPE) (MCA340PE, BioRad) that only labels B-cells. Data were acquired using FACSAria II (Becton Dickinson Immunocytometry Systems, San José, CA, USA) and analyzed using FlowJo 7.6. software (Supplementary Figure S1). Cell viability (99%) was assessed through the Trypan blue exclusion method. LBs isolated were plated in 96-well plates at 1×10^6 cells per well and cultured for 60 h in the presence (LB/IMT504) or absence (LB) of 6 µg/ml IMT504 [26] in RPMI medium. After 60 h, LBs were harvested and washed in SS.

LB Inoculation

LBs were adjusted to 9×10^5 cells/animal and then IV injected through the lateral tail vein, in control (control-LB and control-LB/IMT504) and CPZ-demyelinated animals 48 h after CPZ withdrawal from the diet (CPZ-LB and CPZ-LB/IMT504). At the end of treatment periods, 3 animals per group were sacrificed, as described in the "Toxic CPZ-induced demyelination protocol and IMT504 treatment by subcutaneous (SC) injection" section, 7 days (T7) after inoculation with LBs. The brains were excised and processed for IHC.

Preparation of Tissues for IHC and Electron Microscopy Analysis

Rats were deeply anesthetized as described above and perfused transcardiacally with phosphate-buffered saline, pH 7.4 (PBS) containing 2000 UI/L of heparin solution, followed by 4% (w/v) solution of paraformaldehyde in PBS. The brains were dissected out and post-fixed in the same

solution overnight, followed by thorough washing in PBS and cryoprotection in 30% (w/v) sucrose in PBS. The tissue was then frozen and used to obtain 30-µm free-floating coronal sections using a Leica CM 1850 cryotome.

For electron microscopy, after perfusion, the brains were dissected and 1 × 2 × 1-mm pieces of CC were post-fixed with 2.5% glutaraldehyde, pH 7.4, at 4 °C for 4 h. After washes with 0.1 M phosphate buffer, samples were post-fixed in 1% osmium tetroxide in the same buffer for 60 min at 4 °C. Sections were counterstained with acetate uranyl and lead citrate for 20 min (Reynolds method [40, 41]). G-ratios were calculated as the diameter of the axon divided by the diameter of the axon and myelin.

Immunohistochemistry

For immunohistochemical analyses, cryotome sections were rinsed twice in PBS, pH 7.4, followed by PBS 0.1% Triton (PBST) and blocked for 2 h with a solution containing 1% (w/v) donkey serum in PBST. Sections were incubated overnight at 4 °C with primary antibodies rabbit anti-Sox10 to detect OL lineage cells, goat anti-PDGFRα to detect OPCs, mouse anti-CC1 to detect mature OLs, rabbit anti-MAG to detect myelinating OLs and myelin, goat anti-Iba-1 to detect microglia, and mouse anti-CD68 to detect phagocytic microglia (Supplementary Table 1). In all cases, sections were incubated with fluorescent conjugated anti-rabbit, anti-goat, or anti-mouse secondary antibodies for 2 h (Supplementary Table 2). After immunostaining, cell nuclei were stained with 1 µg/ml Hoechst 33342 as previously described [42]. The dynamic range of the detector was used to determine positive versus background signal, and results were expressed as the number of positive cells per area.

Microscopic Examination

Epifluorescence microscopy analyses were conducted using an Olympus BX50 microscope and photographs were taken with a CoolSnap digital camera. Images were analyzed using ImageJ (National Institutes of Health, Bethesda, MD, USA).

Electronic microscopy analyses were conducted using a MET Zeiss 109 electron microscope and photographs were taken with a Gatan W10000 digital camera.

Primary Cultures of Cortical Microglial Cells and OPCs

Primary cultures of cortical microglial cells and OPCs were prepared as described by McCarthy and de Vellis [43] with modifications. One- to two-day-old pups were sacrificed by decapitation, and their cerebral cortical tissue was dissected. After the removal of meninges, the tissue was dissociated mechanically and plated on poly-D-lysine-coated (0.01 mg/ml) flasks in DMEM/F12 supplemented with 10% (v/v) FBS and 5% CO_2. After 10 to 13 days in culture, cells were shaken at 110 rpm for 2 h to obtain microglia, which were plated in 35-mm 6-well multiwell plates for 24 h, and the culture medium was then replaced with medium with IMT504 (10 µg/ml; IMT504) [44] or without IMT504 (control, C). Microglia cells were cultured in these conditions for another 24 h. Cells were then fixed for ICC or harvested for RNA extraction.

The remaining culture cells were shaken at 200 rpm for 18 h to obtain OPCs, which were placed on poly-D-lysine-coated coverslips with DMEM/F12 supplemented with 10% FBS. After 24 h, OPC culture medium was changed to DMEM/F12 supplemented with 2% B27, FGF-2 (10 ng/ml), and PDGF-AA (10 ng/ml). After 48 h, this medium was changed to the same medium without FGF-2 or PDGF-AA and with IMT504 (10µg/ml; IMT504) or without IMT504 (control, C) and cultured for 2, 4, and 6 days. OPCs were then fixed for ICC.

Immunocytochemistry

OPCs and microglial cells were fixed with 4% paraformaldehyde in PBS for 20 min and then washed twice with PBS. Nonspecific binding was blocked through 30-min incubation in PBS containing 1% donkey serum (Sigma-Aldrich) and 0.1% Triton X-100 at room temperature. OPCs were then incubated for 2 h with the following primary antibodies diluted in blocking solution at room temperature: goat anti-PDGFRα to stain OPCs, mouse anti-myelin basic protein (MBP) to stain mature OLs, and mouse anti-Ki67 to stain proliferating cells (Supplementary Table 1). Microglial cells were incubated for 2 h with goat anti-Iba-1. After PBS washes, cells were incubated for 2 h with fluorescent dye-conjugated secondary antibodies diluted in PBS at room temperature. Secondary antibodies were Cy2- or Cy3-conjugated donkey anti-goat and Cy3-conjugated donkey anti-mouse in combination with 1 µg/ml Hoechst (Supplementary Table 2). After incubations, coverslips were washed twice in PBS and mounted onto glass slides with mounting medium. Microscopic examination was carried out using an Olympus BX50 microscope, and digital images were obtained with a CoolSnap digital camera. Marker-positive cells were counted using ImageJ (Media Cybernetics, Silver Spring, MD, USA), and results were expressed as the percentage of positive cells over total cells. A total of at least 300 cells were counted for each cell marker analyzed in each of the three independent experiments performed in triplicate.

qPCR Analysis

CC was dissected under a magnifier with sterilized material. Tissue and microglial cell samples were kept in sterilized

RNAase-free tubes in an RNA*later* solution (AM7020, Ambion) at 4 °C, immediately frozen and stored at − 80 °C until used. Total RNA was isolated and DNase-treated with the RNAqueous-Micro Kit (AM1931, Ambion) following the manufacturer's instructions. Sample RNA was quantified, and purity was assayed through the A_{260}/A_{280} ratio with a NanoDrop 2000 Spectrophotometer (Thermo Scientific). The amount of RNA obtained from the samples was between 1 and 3 µg, and the A_{260}/A_{280} ratio was between 1.95 and 2.05. One µg of RNA of each sample was used for reverse transcription with random hexamer primers using a High-Capacity cDNA Reverse Transcription Kit (4368814, Applied Biosystems, Waltham, MA, USA) following the manufacturer's instructions and a Veriti 96 Well Thermal Cycler (Applied Biosystems). Glyceraldehyde-3-phosphate dehydrogenase (GAPDH) was used as a housekeeping gene. A total of 5 ng cDNA of each sample was analyzed by qPCR using the Power Up SYBR Green Master Mix (A25742, Applied Biosystems) on a Step One Plus Real-Time PCR System (Applied Biosystems). ROX dye was used as reference to normalize the fluorescence signal of the reporter fluorophore (SYBR green). Primers were designed using Primer Express software and sequences are described in Supplementary Table 3.

The comparative Ct method was used to determine the relative expression levels of each transcript based on raw data from a minimum of three independent experiments. StepOne Software version 2.3 (Applied Biosystems) was used to assess amplification curves for each well and the reliability of results by establishing the Ct and melting curves. A validation experiment was carried out to determine equivalence between target amplification efficiency and reference (GAPDH) amplification efficiency in order to use the ΔΔCt method to calculate fold differences in gene expression across samples. The amount of target, normalized to an endogenous reference and relative to a calibrator, was given by $2^{-\Delta\Delta Ct}$ (RQ).

Statistical Analysis

Data are expressed as the mean ± standard error of the mean (SEM). Assumption of a normal distribution was tested using the Shapiro-Wilks test on the residuals. Comparisons in assays which involved groups along time were made using a general linear model: two-way analysis of variance (ANOVA) for groups and time followed by simple-effects analysis and Di Rienzo-Guzmán-Casanoves (DGC) post hoc tests, a method based on binary trees which achieves groups in disjoint sets [45]. When variance homogeneity was not reached, variance functions were applied on the combination of time points and groups to model the variance structure [46]; the choice of the appropriate variance function (VarIdent or VarExp) was based on the lowest Akaike and Bayesian criteria, which combines the penalization of excessive parameters and the maximization of the likelihood function. Also, the choice was based on the best standardized residuals versus predicted values in a scatter-plot; the best function reached a random distribution of residuals around zero, without structure. When appropriate, group comparisons without time progression were made using two-tailed unpaired Student's *t*-tests or one-way ANOVA. No data points were excluded from the analysis.

InfoStat (Universidad Nacional de Córdoba-Versión 2022) software was used for statistical analysis. Values with $p < 0.05$ were considered statistically significant, except in the variance homogeneity tests, where statistical significance was increased up to 0.10 to minimize type II errors. In each figure, "n" represents the number of animals used for independent cell culture preparations.

Results

Characterization of CPZ Demyelination

Animal body weight was measured every two days across groups along the protocol of IMT504 administration until 2 and 4 days after CPZ withdrawal. Measurements revealed between 21 and 25% lower average body weight in CPZ animals as compared to controls during IMT504 treatment. However, no significant differences were observed between CPZ-SS and CPZ-IMT504 (Supplementary Figure S2A).

In addition, CPZ demyelination was corroborated through Sudan black staining in the CC and striatum at T0, with results showing lower myelin staining in CPZ animals than in controls in both areas (Supplementary Figure S2B).

Effects of SC Treatment with IMT504 on Neuroinflammation Following CPZ Demyelination

PyNTTTTGT ODNs share characteristics with CpG ODNs. For instance, both types directly activate LBs and pDCs. LBs respond to IMT504 by increasing the expression of CD80, CD86, CD40, and MHC-I and II. In addition, LBs secrete IgM and IL-6 and undergo an increase in proliferation [26]. IMT504-stimulated pDCs also increase their co-stimulatory molecules and activation antigens. However, unlike CpG ODNs, PyNTTTTGT ODNs do not induce the production of type I IFN (α and β). Considering the differences between PyNTTTTGT ODNs and CpG ODNs in terms of the biological responses they generate, we evaluated whether these differences involved receptor participation. As TLR9 is considered the receptor of CpG ODNs [46], we used HEK 293-hTLR9 cells to assess TLR9 involvement in ODN activity, as described in the "Methods" section. Results show that HEK 293-hTLR9 cells responded to CpG ODN 2006 stimulation but not to IMT504 stimulation (Supplementary Figure S3).

As previously reported by our group in a rat model [21], the demyelination process induced significant microgliosis in the CC of CPZ-treated animals, as evidenced by a larger number of Iba-1+ cells per area than in controls from T0 to T10. Of note, IMT504 administration succeeded in ameliorating microgliosis as from T3, with significantly fewer Iba-1+ cells in CPZ-IMT504 than in CPZ-SS at T3 and T10 (Fig. 1A, B, and C).

In turn, CPZ-induced demyelination promoted an expansion in the phagocytic microglial population, reflected by a significantly larger number of CD68+Iba-1+ cells in CPZ animals as compared to controls. In addition, CPZ-IMT504 exhibited a reduction in the number of phagocytic microglia at T7 and T10 as compared to CPZ-SS. Most importantly, even if the number of CD68+Iba-1+ cells decreased between T0 and T10 in CPZ animals as a result of spontaneous remyelination, IMT504 administration induced and sharper reduction in both the number of CD68+Iba-1+ cells and their proportion relative to total Iba-1+ microglial cells (Fig. 1D and E). Finally, no differences were observed in the parameters analyzed between control-IMT504 and control-SS animals (Supplementary Figure S4A and B).

Effects of SC Treatment with IMT504 on the Expression of Genes Involved in the Pro- and Anti-inflammatory Response Following CPZ Demyelination in the CC

Taking into account the increase in the population of microglial cells, the expansion of the phagocytic population as a result of demyelination and its more accelerated reduction induced by IMT504 during 5 days before CPZ removal, qPCR analyses were carried out to evaluate mRNA expression of pro-inflammatory genes iNOS and IL-1β and anti-inflammatory genes Arg1 and TGF-β in the CC. Interestingly, and considering that both, control and CPZ-treated animals, received a daily injection of SS or IMT504 during the demyelination process 5 days before CPZ withdrawal, results showed a significant and sharp increase in iNOS (4.4-fold; Fig. 1G) and IL-1β (17-fold; Fig. 1H) transcript levels 1 h after the last IMT504 injection. On the other hand, transcript levels of anti-inflammatory cytokine TGF-β at T0 showed an increase in both CPZ-SS and CPZ-IMT504 (2.2-fold and 3.5-fold, respectively) as compared to control-SS and control-IMT504, with a significant increase in CPZ-IMT504 as compared to CPZ-SS at T0 and T3 (Fig. 1J). No relevant differences were observed across CPZ-SS, CPZ-IMT504, control-SS, and control-IMT504 in Arg1 transcript levels (Fig. 1I). Even if no differences were observed in transcript levels between control-IMT504 and control-SS animals (Supplementary Figure S4E, G, H), IMT504 administration induced a significant increase in the level of IL-1β in the CC of control rats (Supplementary Figure S4F), probably due to the immunomodulatory effect of the ODN on peripheral lymphocytes B. However, this increase was more relevant in the CC of CPZ-demyelinated rats. On the basis of these results and considering that RNA reflects the whole CC and not only the participation of microglia, the effect of IMT504 was further evaluated in primary cultures of microglial cells.

Effects of IMT504 on the Microglial Expression of Genes Involved in the Pro- and Anti-inflammatory Response

Microglial cells were isolated as described in the "Materials and Methods" section and processed according to the experimental design (Fig. 2A). After 24 h in culture, results showed an abrupt change in cell morphology compatible with microglial activation in cells treated with IMT504 as compared to control cells treated with SS (Fig. 2B). Interestingly, qPCR analyses revealed a significant increase in pro-inflammatory iNOS and IL-1β mRNA expression (2.5-fold, Fig. 2C and 2.2-fold, Fig. 2D, respectively) in IMT504-treated cells as compared to control, which is consistent with results obtained in the whole CC. No significant differences were observed in Arg-1or TGF-β transcript levels between IMT504- and SS-treated microglial cells (Fig. 2E and F).

Effects of SC Treatment with IMT504 on the Oligodendroglial Lineage Following CPZ Demyelination

Considering the relevance of early microglial expansion and activation, and, in particular, the phagocytic microglial population for myelin debris clearance and the induction of remyelination, we evaluated the effect of IMT504 administration on the oligodendroglial lineage following CPZ demyelination. IMT504 administration induced two waves of expansion in the OPC population in the CC, as evidenced by a larger number of PDGFRα+ cells in the CPZ-IMT504 group. This expansion was detected at T0 but was even sharper at T7 (Fig. 3A and B).

As expected in CPZ-induced demyelinating conditions, the mature OL population suffered a reduction in the CC of CPZ-SS and CPZ-IMT504 animals, as shown by the smaller number of CC1+Sox10+ cells at T0. As from T3 and up to T10, these cell numbers showed comparable values between experimental conditions (Fig. 3C and D).

In addition, and in keeping with the well-established effects of CPZ intoxication, the myelinating OL population in the CC was sharply reduced at T0, as evidenced by a smaller number of MAG+ cells in both the CPZ-SS and CPZ-IMT504 groups. However, and in agreement with the results obtained in the OPC population, the number of MAG+ OLs gradually recovered and rendered a higher value

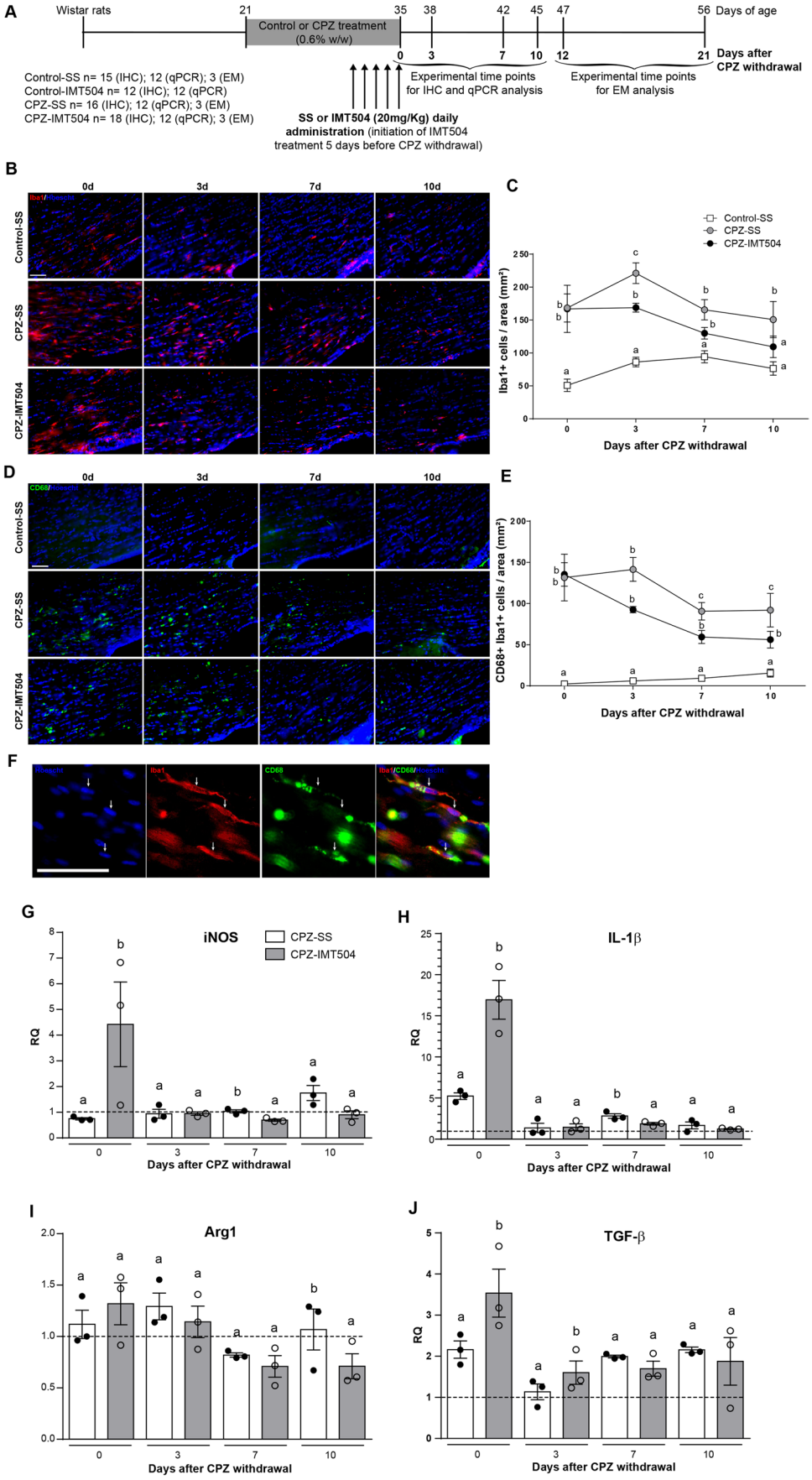

Fig. 1 Effects of SC treatment with IMT504 on neuroinflammation following CPZ demyelination. **A** Experimental timeline. Representative images of **B** Iba-1; **D** CD68; and **F** magnification of Iba-1, CD68, and colocalization of Iba-1/CD68 IHC in the CC of control animals treated with saline solution (Control-SS) and CPZ animals treated with saline solution (CPZ-SS) or IMT504 (CPZ-IMT504) at the different experimental time points. Cell nuclei visualized with Hoechst; scale bar 50 µm. Quantification of **C** Iba-1+ and **E** CD68+Iba-1+ cells per area. Values are expressed as the mean ± SEM. qPCR analyses of **G** iNOS, **H** IL-1β, **I** Arg1, and **J** TGF-β transcript levels in the CC of CPZ-SS and CPZ-IMT504 animals at the different experimental time points. Results are expressed as RQ fold changes regarding controls (dotted lines). Values are expressed as the mean ± SEM. Statistical analysis was done using two-way ANOVA and Di Rienzo-Guzmán-Casanoves post-test as described in the "Materials and Methods" section; different letters indicate significant differences, $p < 0.05$. IHC, immunohistochemistry

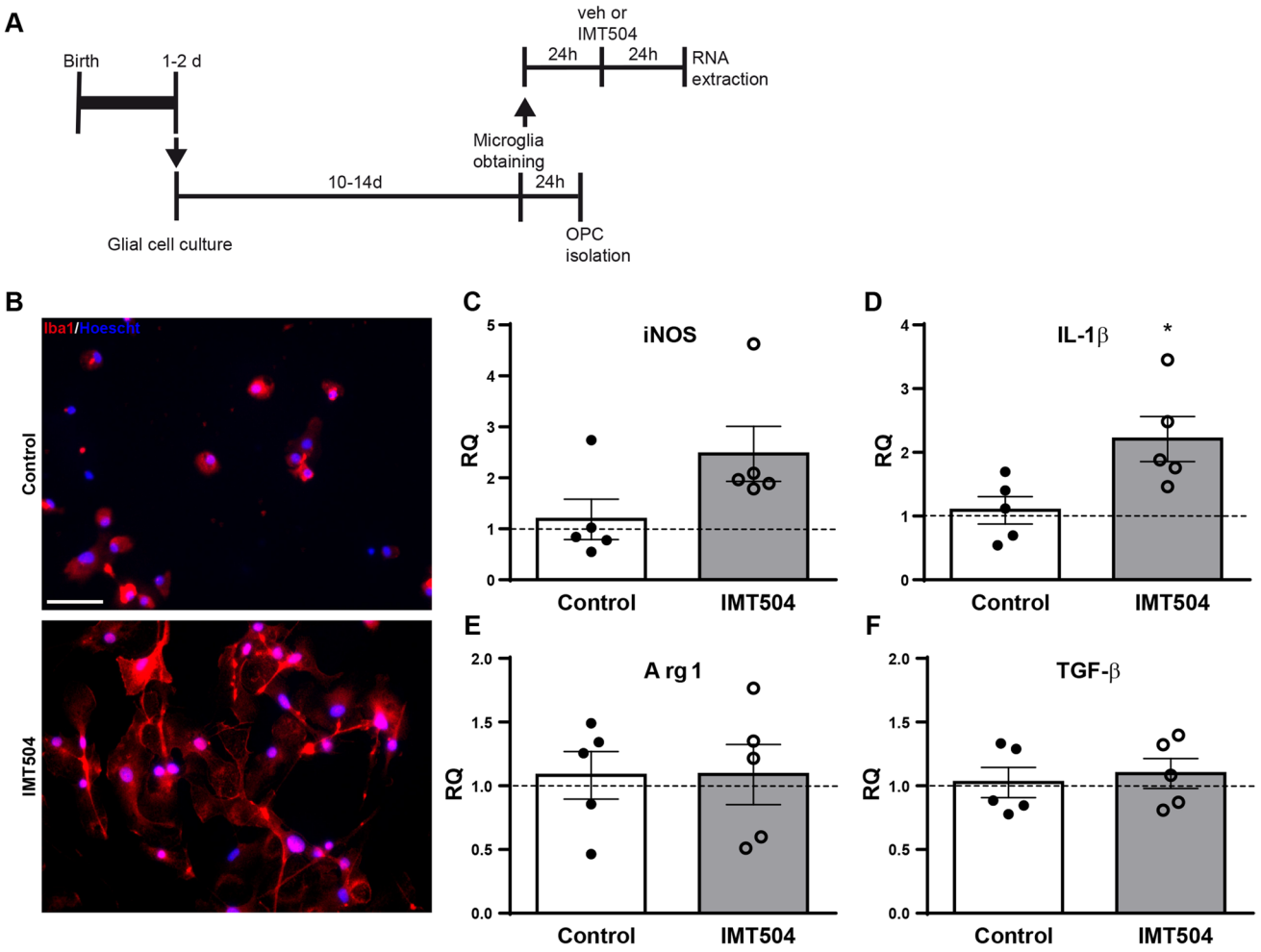

Fig. 2 Effects of IMT504 on the microglial expression of genes involved in the pro- and anti-inflammatory response. **A** Experimental timeline. **B** Representative images of Iba-1 ICC of control and IMT504-treated microglial cells. qPCR analyses of **C** iNOS, **D** IL-1β, **E** Arg1, and **F** TGF-β transcript levels in control and IMT504-treated microglial cells. Results are expressed as RQ fold changes regarding controls (dotted lines). Values are expressed as the mean ± SEM. Statistical analysis was done using two-tailed unpaired Student's *t*-tests as described in the "Materials and Methods" section; *p<0.05. ICC: immunocytochemistry

in the CPZ-IMT504 group as from T3 (Fig. 3E and F), following the expansion of PDGFRα+ OPCs described above. Finally, no differences were observed in the parameters analyzed between control-IMT504 and control-SS animals (Supplementary Figure S4C and D).

Having characterized the proportion of cells at different stages of the oligodendroglial lineage in the CC of CPZ-treated animals after receiving SS or IMT504, qPCR analyses were carried out to determine the transcript levels of PDGFRα, MAG and MBP genes. Results revealed a significant increase in PDGFRα transcript levels at T0 and T7 (2.1 and 1.7-fold respectively) in CPZ-IMT504 as compared to CPZ-SS. In addition, MAG and MBP transcript levels increased at T10 (1.8-fold) and T7 (2.0-fold), respectively, in the CC of CPZ-IMT504 animals as compared to control-SS (Fig. 3H, I and J). No differences were observed in the parameters analyzed between control-IMT504 and control-SS animals (Supplementary Figure S4I, J and K).

These results are in agreement with immunohistochemical findings; indeed, the expansion in the OPC population at T0 and T7 appeared to result from the increase in PDGFRα transcript levels, while the expansion in the population of mature myelinating OLs at T10 seemed to respond to the increase in MBP and MAG mRNA expression at T7 and T10, respectively. The higher MAG transcript levels observed at T0 in the CPZ-IMT504 group as compared to CPZ-SS may, in turn, respond to the pro-differentiating effects of the ODN.

On the basis of these results, we assessed remyelination in the CC of control, CPZ-SS, and CPZ-IMT504 animals by calculating the mean g-ratio (the ratio of the inner axonal diameter to the total outer diameter) through electron microscopy.

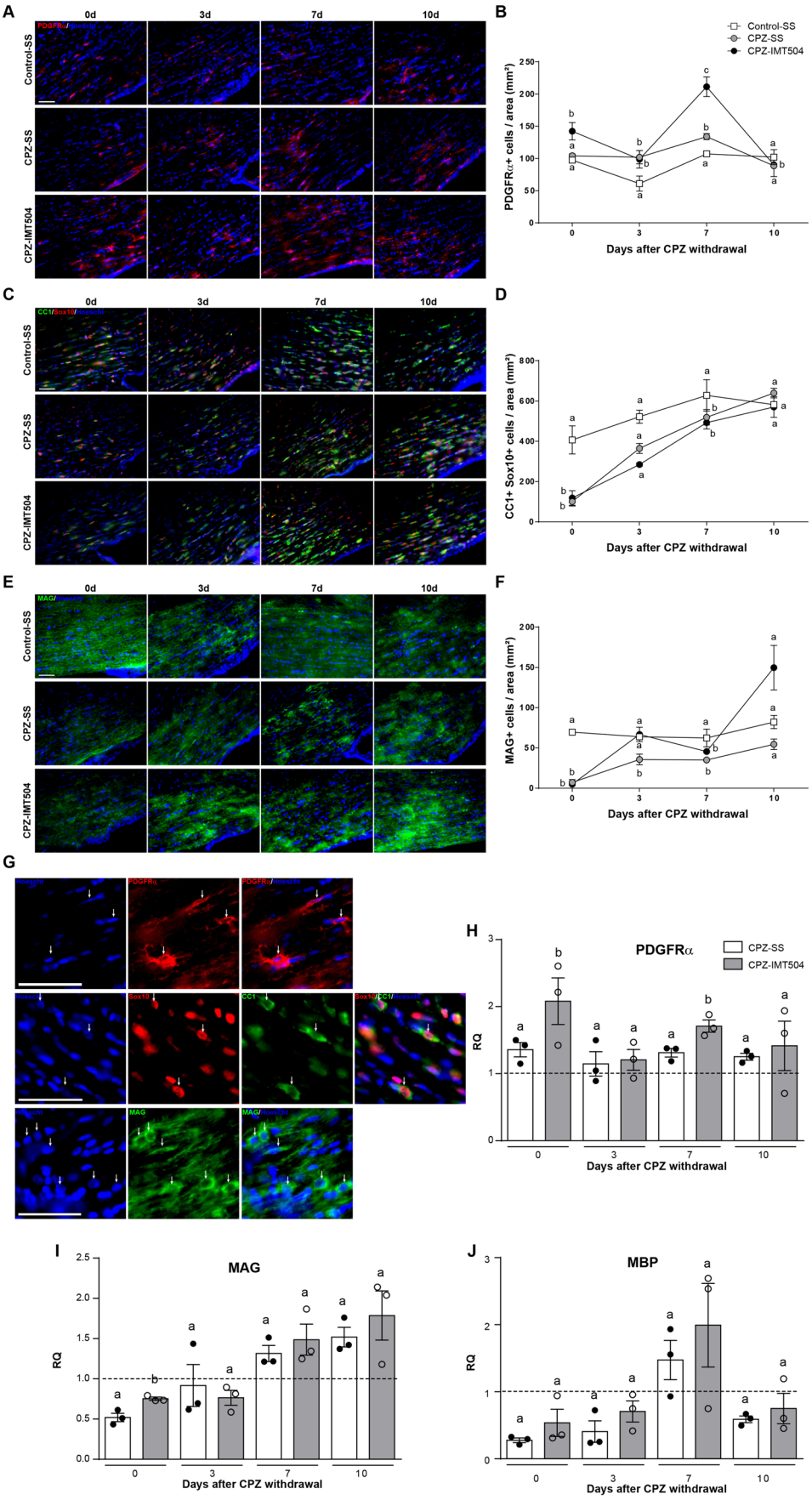

Fig. 3 Effects of SC treatment with IMT504 on the oligodendroglial lineage following CPZ demyelination. Representative images of **A**, PDGFRα, **C** CC1, and Sox10, **E** MAG, and **G** magnification of PDGFRα, CC1, Sox10, CC1/Sox10 colocalization, and MAG IHC in the CC of control animals treated with saline solution (Control-SS) and CPZ animals treated with saline solution (CPZ-SS) or IMT504 (CPZ-IMT504) at different experimental time points; cell nuclei visualized with Hoechst; scale bar 50 µm. Quantification of **B** PDGFRα+, **D** CC1+Sox10+, and **F** MAG+ cells per area. Values are expressed as the mean ± SEM. qPCR analyses of **H** PDGFRα, **I** MAG, and **J** MBP transcript levels in the CC of CPZ-SS and CPZ-IMT504 animals at different experimental time points. Results are expressed as RQ fold changes regarding controls (dotted lines). Values are expressed as the mean ± SEM. Statistical analysis was done using two-way ANOVA and Di Rienzo-Guzmán-Casanoves post-test as described in the "Materials and Methods" section; different letters indicate significant differences, $p < 0.05$. IHC, immunohistochemistry

A typical g-ratio for a normally myelinated axon is between 0.6 and 0.8 [47, 48], while a g-ratio of 1.0 indicates complete demyelination. Analyses were conducted on 3 animals from each experimental group at T12 and T21 after CPZ removal, with results showing a significantly higher g-ratio in CPZ-SS than in control or CPZ-IMT504 animals and suggesting a pro-myelinating effect of IMT504 (Fig. 4A and B).

Given that these results may reflect a direct effect of IMT504 on the oligodendroglial cell lineage, the impact of microglial cell activation, or peripheral LB activation by the ODN, further studies were conducted on the effect of IMT504 on primary OPC cultures.

Effects of IMT504 on OPC Cultures

OPCs were isolated as described in the "Materials and Methods" section and processed according to the experimental design (Fig. 5A). After 48 h in culture with specific medium, OPCs were incubated without growth factors FGF-2 and PDGF-AA and in the presence or absence of IMT504 for 2, 4, or 6 days. As compared to T0, the presence of IMT504 produced a significant decrease in the percentage of PDGFRα+ OPCs after 4 days in culture, whereas, in the absence of IMT504, this decrease was observed only after 6 days in culture. Along the same line, results showed a significant increase in the percentage of mature, myelinating MBP+ OLs in 4-and 6-day cultures stimulated with IMT504 as compared to T0 (Fig. 5B, D and E). Furthermore, assays on Ki67+ cells revealed no impact of IMT504 on OPC proliferation (Fig. 5B, F and G) suggesting that OPC expansion observed in the CC of demyelinated animals could be due to the microglial cell activation and consequently the increased in IL-1β induced by IMT504. In other words, other than its impact on microglial cell activation and peripheral LB activation in in vivo experiments, IMT504 appears to have a direct effect on OPC maturation in culture.

Effects of IC Treatment with IMT504 on Neuroinflammation and Oligodendroglial Cell Population Following CPZ Demyelination

Experiments were also conducted to further characterize IMT504 effects following CPZ demyelination. Franco et al. [30] demonstrated that the level of IMT504 increases quickly in plasma upon SC administration, while ODN passage

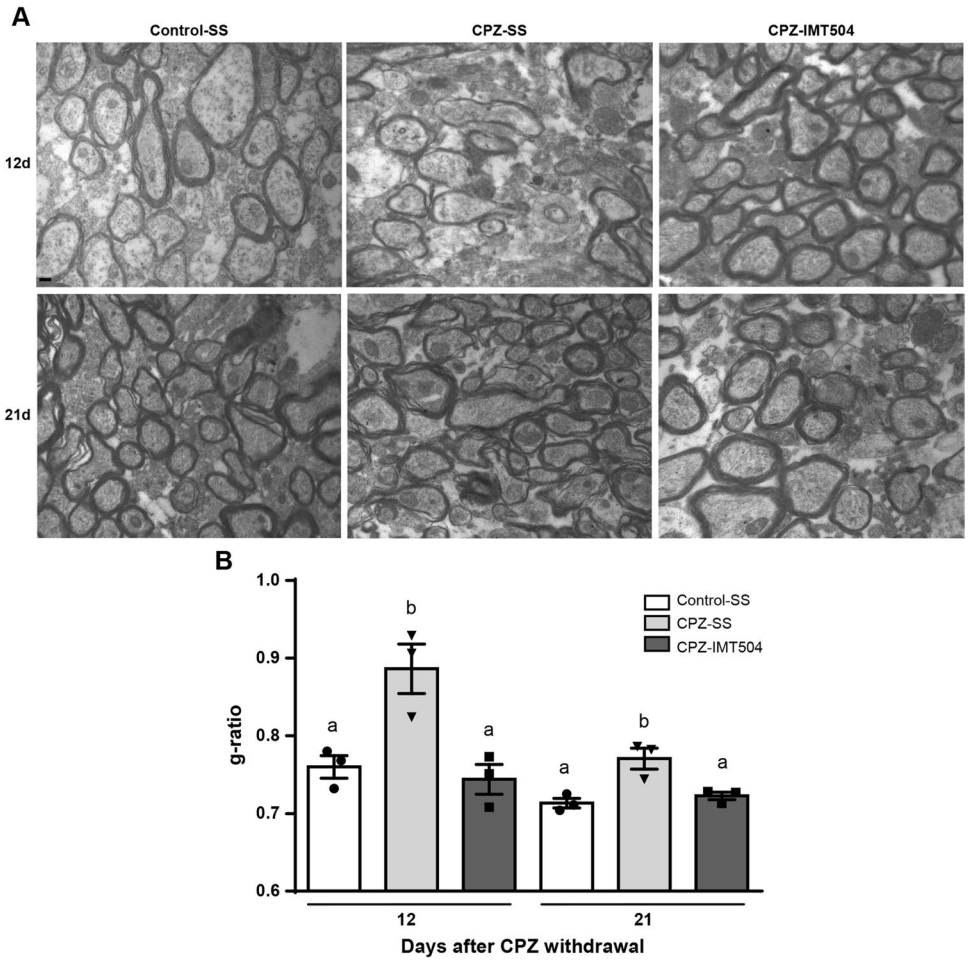

Fig. 4 Effects of SC treatment with IMT504 on CC remyelination. **A** Representative electron microscopy images of the CC of control animals treated with saline solution (Control-SS) and CPZ animals treated with saline solution (CPZ-SS) or IMT504 (CPZ-IMT504) at T12 and T21. Scale bar 0.2 µm. **B** Quantification of the degree of remyelination. Results are expressed as the g-ratio. Values are expressed as the mean ± SEM. Statistical analysis was done using two-way ANOVA and Di Rienzo-Guzmán-Casanoves post-test as described in the "Materials and Methods" section; different letters indicate significant differences, $p < 0.05$

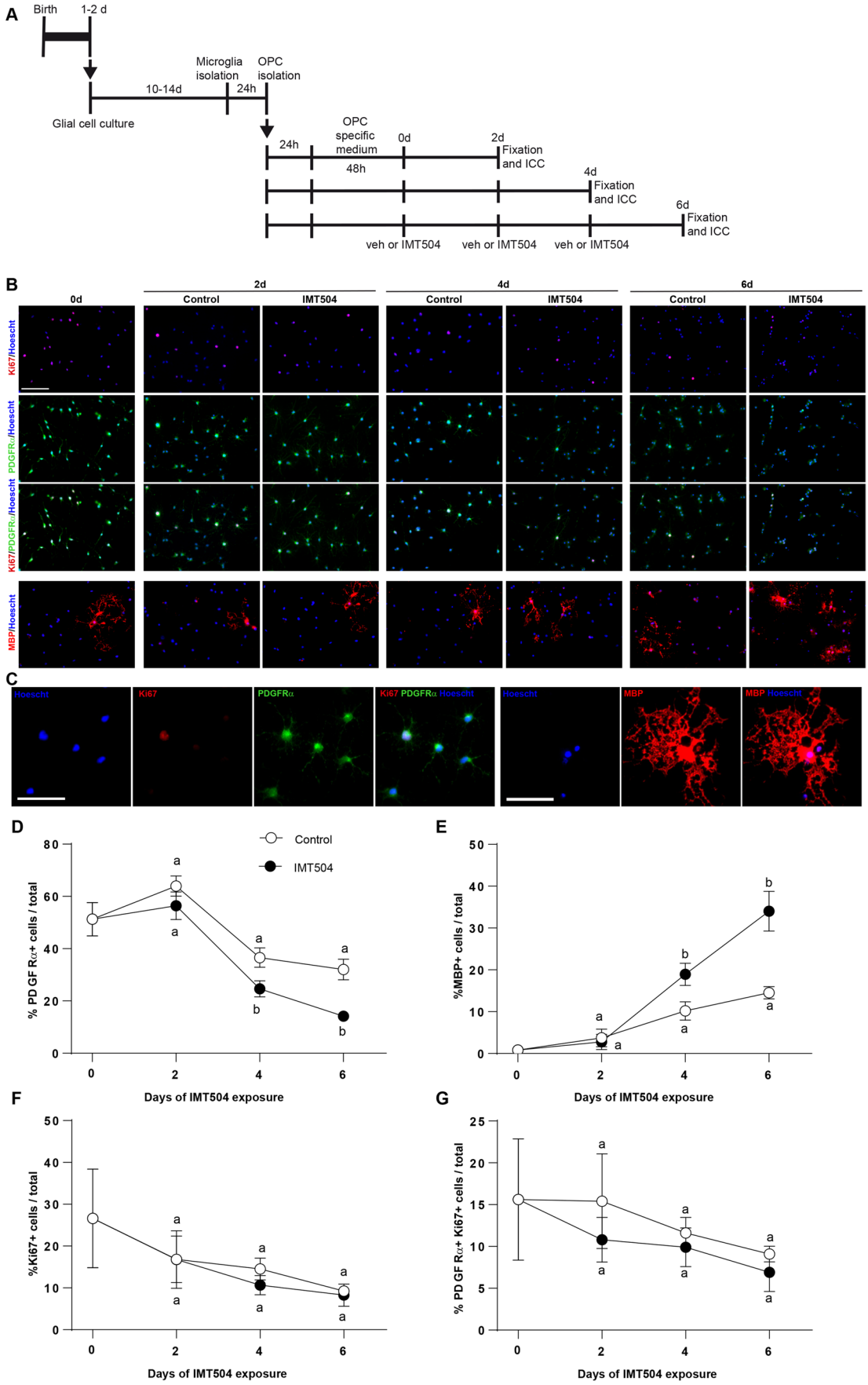
A
Birth
1-2 d
Microglia isolation
OPC isolation
10-14d
24h
Glial cell culture
24h
OPC specific medium
48h
0d
2d
Fixation and ICC
4d
Fixation and ICC
6d
Fixation and ICC
veh or IMT504
veh or IMT504
veh or IMT504
B
0d
2d
4d
6d
Control
IMT504
Ki67/Hoescht
PDGFRα/Hoescht
Ki67/PDGFRα/Hoescht
MBP/Hoescht
C
Hoescht
Ki67
PDGFRα
Ki67 PDGFRα Hoescht
Hoescht
MBP
MBP Hoescht
D
Control
IMT504
% PD GF Rα+ cells / total
Days of IMT504 exposure
E
%MBP+ cells / total
Days of IMT504 exposure
F
%Ki67+ cells / total
Days of IMT504 exposure
G
% PD GF Rα+ Ki67+ cells / total
Days of IMT504 exposure

◂**Fig. 5** Effects of IMT504 on OPC cultures. **A** Experimental timeline. **B** Representative images of Ki67, PDGFRα and MBP ICC of control and IMT504-treated OPCs at the different experimental time points. **C** Magnification of Ki67, PDGFRα, Ki67/PDGFRα colocalization, and MBP. Quantification of relative percentages of **D** PDGFRα+, **E** MBP+, **F** Ki67+, and **G** PDGFRα+ Ki67+ over total cells visualized with Hoechst. Values are expressed as the mean ± SEM of three independent experiments performed in triplicate. Statistical analysis was done using two-tailed unpaired Student's *t*-tests as described in the "Materials and Methods" section; different letters indicate significant differences compared to 0 d, $p < 0.05$. ICC, immunocytochemistry

through the blood-brain barrier is minimal. In addition, it has been shown that both CpG and Non-CpG ODNs target B-cells. For these reasons, we wondered whether IMT504 effects on the CNS might be direct, systemic, or both, and thus studied the effects of IMT504 administration by stereotaxic injection into the CC of CPZ-treated animals. Results showed a significant recruitment and expansion of both the population of Iba-1+ cells 3 days after IC IMT504 administration and the phagocytic subpopulation of CD68+/Iba-1+ cells 3 and 10 days after IMT504 injection in the ipsilateral as compared to the contralateral region of the CC of CPZ-treated animals (Fig. 6A–E). A larger number of PDGFRα+ cells was observed in the ipsilateral than in the contralateral region 7 days after IMT504 injection, and an expansion of the MAG+ cell population was detected 10 days after injection (Fig. 6F–H). These results showing the action of IC IMT504 on microglial cells, OPCs and OLs in the CC of CPZ-demyelinated animals, together with those obtained in microglial and OPC culture treatments, reinforce the notion that the ODN exerts, at least in part, direct effects on these CNS glial cells.

Effects of IV Inoculation of Isolated LB Treated with IMT504 on Neuroinflammation and Oligodendroglial Cell Population Following CPZ Demyelination

Considering that LB are target cells of ODNs, we analyzed the effect of LB isolated from young adult rats and treated with IMT504 (LB/IMT504) or vehicle (LB) in control and CPZ-demyelinated animals. Results showed that the IV administration of IMT504, LB, and IMT504-treated LB significantly reduced the number of Iba-1+ and phagocytic CD68+Iba-1+ cells per area in the CC of CPZ-demyelinated rats 7 days after the inoculation (Fig. 7B and C) as compared to the CPZ-SS group. On the other hand, only the IV injection of IMT504 significantly increased the number of PDGFRα+ cells (Fig. 7D), whereas the IV administration of IMT504 and IMT504-treated LB significantly expanded the number of MAG+ cells in the CC of CPZ-demyelinated (Fig. 7E). No changes were observed in the population of CC1+Sox10+ cells (Fig. 7F). Despite differences in experimental designs, these findings on the effect of IMT504-treated LB on the microglial, OPC, and mature OL populations may be thought to correlate with the results obtained in SC administration assays and suggest a partly direct, partly systemic effect of IMT504.

Discussion

Demyelinating disorders are characterized by neurodegeneration resulting from incomplete remyelination. In particular, MS is the most common demyelinating disease, affecting more than two million people worldwide [39]. MS is characterized by foci of CNS demyelination and axonal damage as a consequence of persistent brain and spinal cord inflammation caused by the infiltration of immune cells through the compromised blood-brain barrier [49].

ODNs are synthetic molecules which stimulate the immune system and can be classified on the basis of their CpG content as CpG ODNs [50] and non-CpG ODNs [22]. IMT504, a non-CpG ODN, is characterized by both its immunomodulatory effects and its regenerative properties [51]. Unmethylated CpG DNA has been identified as a TLR9 agonist. In addition, the complexity of TLR roles in the pathogenesis of MS may lie in their ability to promote or suppress autoimmune diseases. Studies have shown that mice deficient in MyD88, an adaptor protein for all TLRs except TLR3, are resistant to EAE, and that TLR9 mediates pathogenesis in this model [23]. On the other hand, TLR4- and TLR9-deficient mice exhibit more severe EAE symptoms than those observed in wild type mice, with regulatory roles for TLR4 and TLR9 [52]. We demonstrate here that, despite the common features of PyNTTTTGT and CpG ODNs, HEK 293-hTLR9 cells did not respond to IMT504 stimulation. In this context, IMT504 could be thought to have promyelinating effects by either modulating microglial polarization between different phenotypes and their phagocytic capacity or regulating the proliferation of OPCs or their differentiation. Building on this evidence, the present work further characterizes the effects of IMT504 on neuroinflammation and the oligodendroglial cell population following CPZ demyelination in rats.

Regarding experimental models of demyelination, those induced by toxicants pose the advantage of triggering a spontaneous myelin repair process upon toxicant removal, thus allowing the study of remyelination mechanisms [53]. In particular, CPZ demyelination has been studied and characterized in vivo in mice [54]. Previous work by our group has demonstrated substantial CNS myelin damage in rats 2 weeks after CPZ implementation [19] and an inflammatory response to CPZ in the CC characterized by both microgliosis and astrogliosis [21]. CPZ-induced demyelination is thus a suitable model to mimic MS pattern-III lesions,

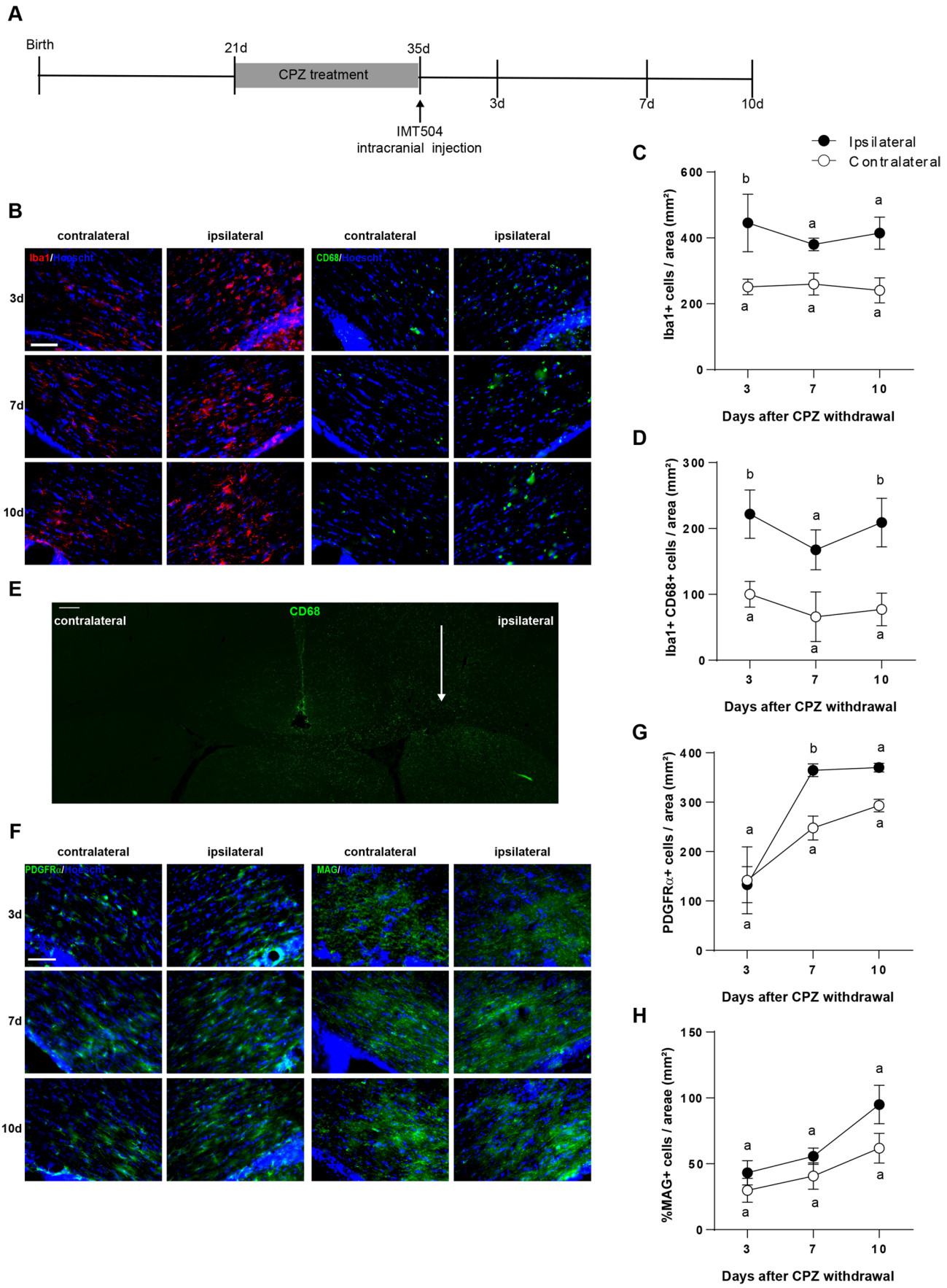
A
Birth
21d
35d
CPZ treatment
3d
7d
10d
IMT504
intracranial injection
B
contralateral
ipsilateral
contralateral
ipsilateral
Iba1/Hoescht
CD68/Hoescht
3d
7d
10d
C
Ipsilateral
Contralateral
Iba1+ cells / area (mm²)
Days after CPZ withdrawal
D
Iba1+ CD68+ cells / area (mm²)
Days after CPZ withdrawal
E
CD68
contralateral
ipsilateral
F
contralateral
ipsilateral
contralateral
ipsilateral
PDGFRα/Hoescht
MAG/Hoescht
3d
7d
10d
G
PDGFRα+ cells / area (mm²)
Days after CPZ withdrawal
H
%MAG+ cells / areae (mm²)
Days after CPZ withdrawal

◂**Fig. 6** Effects of IC treatment with IMT504 on neuroinflammation and oligodendroglial cell population following CPZ demyelination. **A** Experimental timeline. Representative images of **B** Iba-1 and CD68, **F** PDGFRα and MAG IHC in the ipsilateral and contralateral areas of the CC of CPZ animals treated with IMT504 at different experimental time points. Cell nuclei visualized with Hoechst; scale bar 50 µm. **E** Representative image of CD68 IHC (low magnification); scale bar 250 µm; arrow indicates the injection site. Quantification of **C** Iba-1+, **D** CD68+Iba-1+, **G** PDGFRα, and **H** MAG cells per area. Values are expressed as the mean ± SEM. Statistical analysis was done using two-way ANOVA and Di Rienzo-Guzmán-Casanoves post-test as described in the "Materials and Methods" section; different letters indicate significant differences, $p < 0.05$

characterized by OL apoptosis and early MAG downregulation [4]. Furthermore, ODN IMT504 has shown immunomodulatory and tissue repair properties, and its safety has been demonstrated through pharmacokinetics and toxicity studies in rats and monkeys, using single or repeated doses and different routes of administration such as SC or IV [34]. Given that the maximum dose tolerated in rats was determined to be 50 mg/kg when administered SC [34], and considering in vivo studies on neuropathic pain [29–31], we evaluated the effects of SC administration of 20 mg/kg IMT504 on neuroinflammation following CPZ demyelination.

As regards the inflammatory response and in agreement with our previous study in rats [21], CPZ treatment rendered an increase in the number of microglial cells in the CC, in particular phagocytic CD68+Iba-1+ microglia, during acute demyelination. Although all CPZ-treated rats showed a decrease in the number of phagocytic microglia after toxicant removal, this decrease was detected earlier and significantly sharper in CPZ-IMT504 than in CPZ-SS animals during spontaneous remyelination process.

Considering these effects of IMT504, qPCR analyses were carried out on transcript levels of pro-inflammatory genes iNOS and IL-1β and anti-inflammatory genes Arg1 and TGF-β in the CC. Interestingly, although both control and CPZ animals received a daily injection of IMT504 or SS 5 days before CPZ withdrawal, we observed a significant and marked increase in iNOS and IL-1β transcript levels one hour after the last injection of IMT504 in CPZ-IMT504 animals. Surprisingly, IL-1β also showed a significant increase in control-IMT504 animals. Although transcript levels of anti-inflammatory cytokine TGF-β showed an increase in both CPZ-SS and CPZ-IMT504 as compared to control-SS and control-IMT504, the increase was more prominent in CPZ-IMT504. However, no significant differences were observed across groups in Arg1 transcript levels. Interestingly, a significant increase in pro-inflammatory IL-1β mRNA expression was also observed in IMT504-treated microglial cell cultures as compared to control, which is consistent with results obtained in the whole CC.

It should be highlighted that CNS disorders such as MS or amyotrophic lateral sclerosis are characterized by chronic activation of microglial cells [16, 55, 56], and that the loss of homeostasis and the activation of glial cells play essential roles in the progression of demyelination and neurodegeneration. Therefore, the resolution of the microglial pro-inflammatory state through the transition to an anti-inflammatory state becomes crucial. In this work, the immunomodulatory effect of IMT504 seemed to exacerbate the pro-inflammatory response to demyelination induced by CPZ treatment, essential to myelin debris clearance, and to accelerate the transition to the anti-inflammatory state. Even though results obtained at T3, T7, and T10 are not indicative of a residual effect of IMT504 on iNOS, IL-1β, TGF-β, or Arg1 expression, the ODN does seem to have influenced the oligodendroglial lineage. This is in line with evidence of the interaction between glial cells and its effects on OPCs and mature OLs participating in the demyelination-remyelination process through a complex mechanism involving different signaling pathways [57]. Whereas most OPCs differentiate to mature and myelinating OLs during development, 5–8% glial cells in the adult brain remain OPCs [11, 58] with differentiation capacity in conditions of myelin turnover or in response to demyelination. In the present work, ODN administration results showed two waves of OPC expansion as a consequence of demyelination, i.e., upon CPZ withdrawal and 7 days later. Accordingly, IMT504 induced an increase in mature OLs from 3 to 10 days after CPZ removal, a finding supported by PDGFRα and MAG transcript levels. This effect may result from a direct effect of IMT504 on OPCs or an action mediated by microglial activation as reflected by the increase in IL-1β. Of note, the latter may be thought to partly recapitulate the mechanisms of developmental myelination, with IL-1β promoting oligodendrogenesis [59, 60]. This remyelinating action finds further support in electron microscopy results showing a decrease in the g-ratio of animals receiving SC IMT504. Nevertheless, given the direct impact of IMT504 on OPCs in culture, a combination of both effects cannot be ruled out.

In addition, it has also been demonstrated that PyNTTT TGT ODNs are efficient activators of B cells and null inducers of IFNα [26, 61], and that they increase the number of mesenchymal stem cell precursors in vitro and in vivo, thus inducing animal tissue repair [27]. In order to evaluate whether IMT504 impact on CC neuroinflammation and oligodendroglial cells resulted from a direct mechanism or peripheral LB activation, we further studied the effect of IC IMT504 administration 3, 7, and 10 days after stereotaxic injection. An increase was observed in total and phagocytic microglia in the ipsilateral as compared to the contralateral region of the CC, followed by an early expansion of the OPC population and a later increase in mature OLs. Although peripheral effects of IMT504 cannot be disregarded, our

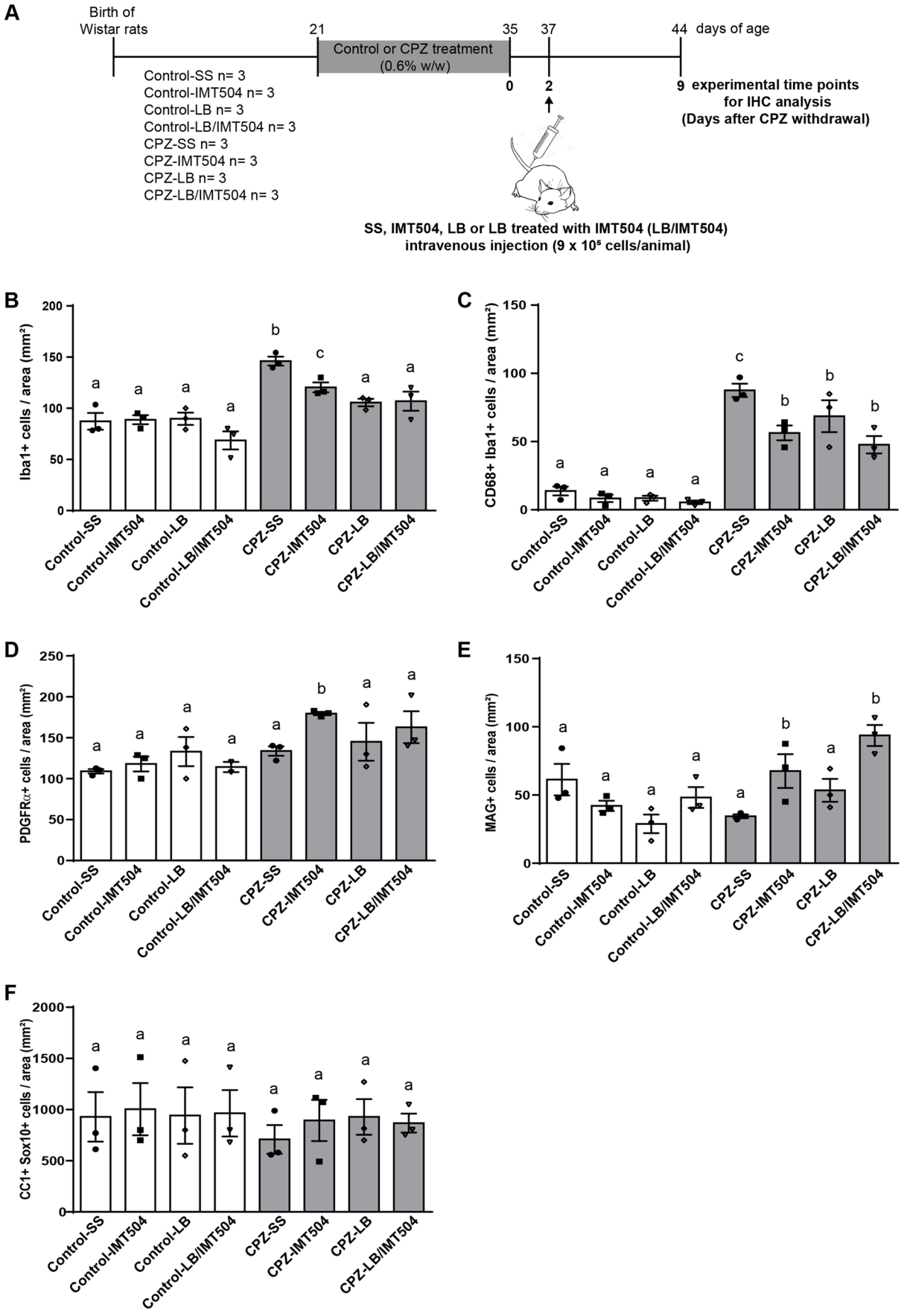
A
Birth of Wistar rats
21
35
37
44 days of age
Control or CPZ treatment (0.6% w/w)
Control-SS n= 3
Control-IMT504 n= 3
Control-LB n= 3
Control-LB/IMT504 n= 3
CPZ-SS n= 3
CPZ-IMT504 n= 3
CPZ-LB n= 3
CPZ-LB/IMT504 n= 3
0
2
9 experimental time points for IHC analysis (Days after CPZ withdrawal)
SS, IMT504, LB or LB treated with IMT504 (LB/IMT504) intravenous injection (9 x 10⁵ cells/animal)
B
Iba1+ cells / area (mm²)
C
CD68+ Iba1+ cells / area (mm²)
D
PDGFRα+ cells / area (mm²)
E
MAG+ cells / area (mm²)
F
CC1+ Sox10+ cells / area (mm²)
Control-SS
Control-IMT504
Control-LB
Control-LB/IMT504
CPZ-SS
CPZ-IMT504
CPZ-LB
CPZ-LB/IMT504

◂**Fig. 7** Effects of IV administration of isolated LB treated with IMT504 on neuroinflammation and oligodendroglial cell population following CPZ demyelination. **A** Experimental timeline. Quantification of **B** Iba-1+, **C** CD68+Iba-1+, **D** PDGFRα+, **E** MAG+, and **F** CC1+Sox10+ cells per area in the CC of control animals treated with saline solution (Control-SS), IMT504 (Control-IMT504), LB (Control-LB) or LB treated with IMT504 (Control-LB/IMT504) and CPZ animals treated with saline solution (CPZ-SS), IMT504 (CPZ-IMT504), LB (CPZ-LB) or LB treated with IMT504 (CPZ-LB/IMT504). Values are expressed as the mean ± SEM. Statistical analysis was done using one-way ANOVA and Bonferroni's post-test as described in the "Materials and Methods" section; different letters indicate significant differences compared to Control-SS and CPZ-SS, $p < 0.05$

results indicate that IMT504 action on microglial cells, OPCs, and OLs could be, at least in part, a direct effect on CNS cells which is not mediated by TLR9.

We further analyzed the effects of LB isolated from adult rats and treated with IMT504 or its vehicle, with results showing that the IV administration of IMT504, LB, and IMT504-treated LB significantly reduced the number of Iba-1+ and phagocytic CD68+Iba-1+ microglial cells in the CC of CPZ-demyelinated rats as compared to the CPZ-SS group. Interestingly, IV administration of IMT504 and IMT504-treated LB significantly expanded the number of MAG+ mature OLs in the CC of CPZ-demyelinated animals. Of note, several of MS risk single-nucleotide polymorphisms (SNPs) are in or near genes for co-stimulatory molecules playing a role in B cells in the context of antigen presentation and T cell activation, such as CD40 and CD86 [62]. Moreover, it has been demonstrated that ODNs containing a PyNTTTTGT motif stimulate the proliferation of B cells and the expression of cell surface molecules CD86, CD40, MHC I, and MHC II [26]. Future experiments will thus be conducted to explore the relevance of this property of IMT504 in the remyelination process as well as the potential direct or cell-mediated effect of IMT504 in other neuroinflammation models. Despite differences in experimental designs, these findings on the effect of IMT504-treated LB on the microglial, OPC, and mature OL populations correlate with the results obtained in SC administration assays and suggest a partly direct, partly systemic effect of IMT504.

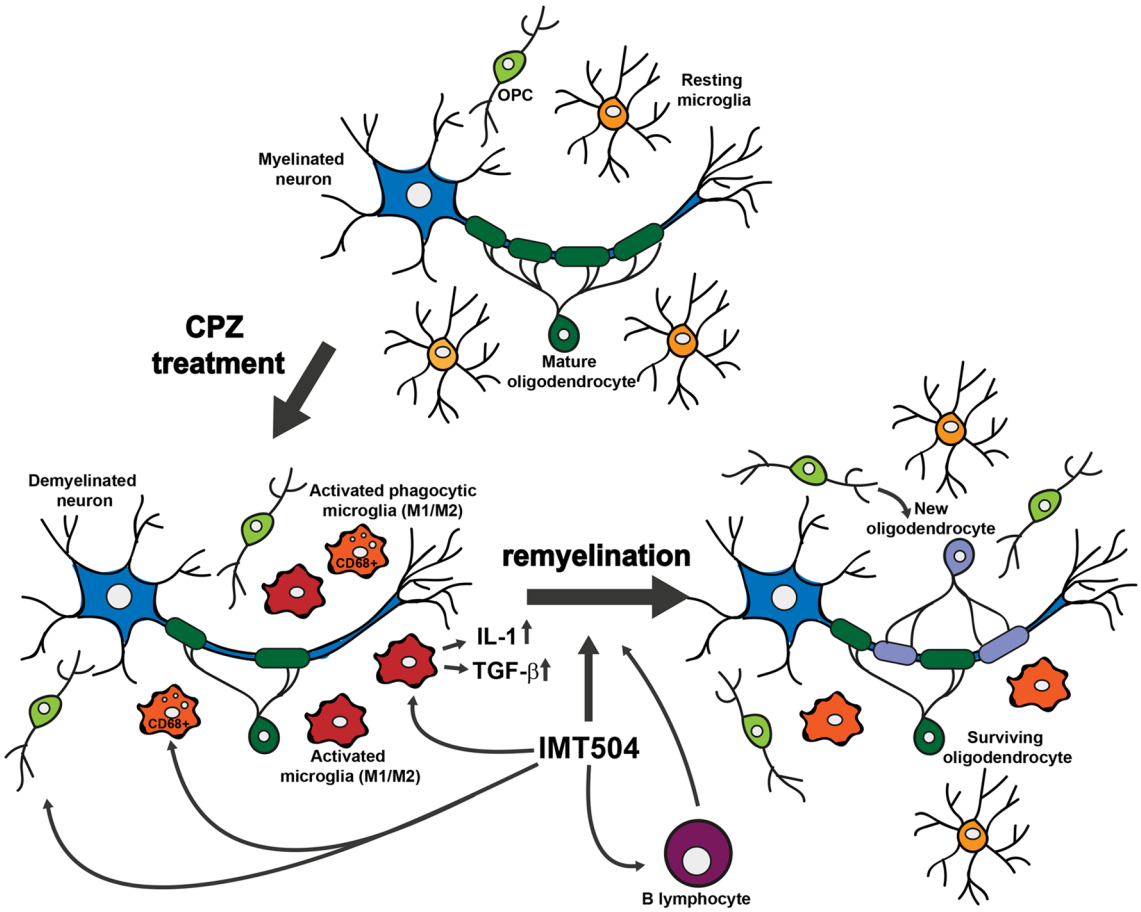

Fig. 8 CPZ administration produced CC demyelination and induced microgliosis in rats. IMT504 induced an expansion of the CD68+ phagocytic microglial population and accelerated the transition to an anti-inflammatory state, ameliorating microgliosis, reducing microglial phagocytic capacity, and inducing an increase in the proportion of mature OLs. The same effect was observed after the inoculation of IMT504-treated LB. These results show more effective CC remyelination as a consequence of IMT504 treatment

Although these assays focused on the CC of CPZ-treated rats, in line with previous results [19, 21], we are now expanding our analysis to other areas of the CNS which are also affected in the CPZ model and whose lesions have been observed in MS, MOG antibody-associated disorder, and neuromyelitis optica spectrum disorder, once considered a sub-type of MS and characterized by brain demyelinating lesions and optic nerve inflammation [63].

In sum, the present work unveils potentially beneficial properties of IMT504 in the regulation of neuroinflammation, oligodendrogenesis, and remyelination. These findings, together with compelling evidence of IMT504 safety, reinforce the clinical potential of this ODN and may be of great relevance in the development of therapeutic strategies for demyelinating and inflammatory diseases such as MS, Neuromyelitis optica spectrum disorder (Fig. 8).

Supplementary Information The online version contains supplementary material available at https://doi.org/10.1007/s12035-023-03825-7.

Author Contribution P.A.M. and Y.R.S. performed most of the experiments. F.E. performed the isolation and culture of LB. A.S.S carried out microglial and OPC culture experiments. P.A.M. and A.M.A. designed and supported all the experiments. M.L.C contributed with statistical analysis. R.L. collaborated with the discussion of this paper. A.M.A. wrote the manuscript.

Funding Supported by grants from ANPCyT (PICT 2017-0890), Universidad de Buenos Aires (20020160100050BA) and CONICET (PIP0567), Argentina.

Data Availability The datasets generated during the current study are not publicly available but are available from the corresponding author on reasonable request.

Declarations

Ethics Approval Experiments were carried out following the guidelines of the Institutional Committee for the Care and Use of Laboratory Animals, Facultad de Farmacia y Bioquímica, Universidad de Buenos Aires, approved by Council Directive (CICUAL; CUDAP:EXP-FYB 0043071/2019). This study was exploratory and was not pre-registered.

Consent to Participate Not applicable.

Consent to Publish Not applicable.

Conflict of Interest The authors declare no competing interests.

References

1. Noseworthy JH, Lucchinetti C, Rodriguez M, Weinshenker BG (2000) Multiple sclerosis. N Engl J Med 343:938–952
2. Ramagopalan SV, Deluca GC, Degenhardt A, Ebers GC (2008) The genetics of clinical outcome in multiple sclerosis. J Neuroimmunol 201-202:183–199
3. Trapp BD, Nave KA (2008) Multiple sclerosis: an immune or neurodegenerative disorder? Annu Rev Neurosci 31:247–269
4. Vega-Riquer JM, Mendez-Victoriano G, Morales-Luckie RA, Gonzalez-Perez O (2019) Five decades of cuprizone, an updated model to replicate demyelinating diseases. Curr Neuropharmacol 17:129–141
5. Jeffery ND, Blakemore WF (1997) Locomotor deficits induced by experimental spinal cord demyelination are abolished by spontaneous remyelination. Brain 120(Pt 1):27–37
6. Liebetanz D, Merkler D (2006) Effects of commissural de- and remyelination on motor skill behaviour in the cuprizone mouse model of multiple sclerosis. Exp Neurol 202:217–224
7. Franklin RJM, Frisen J, Lyons DA (2021) Revisiting remyelination: towards a consensus on the regeneration of CNS myelin. Semin Cell Dev Biol 116:3–9
8. Grinspan JB (2020) Inhibitors of myelination and remyelination, bone morphogenetic proteins, are upregulated in human neurological disease. Neurochem Res 45:656–662
9. Sabo JK, Aumann TD, Merlo D, Kilpatrick TJ, Cate HS (2011) Remyelination is altered by bone morphogenic protein signaling in demyelinated lesions. J Neurosci 31:4504–4510
10. Huang JK, Fancy SP, Zhao C, Rowitch DH, Ffrench-Constant C, Franklin RJ (2011) Myelin regeneration in multiple sclerosis: targeting endogenous stem cells. Neurotherapeutics 8:650–658
11. Dawson MR, Polito A, Levine JM, Reynolds R (2003) NG2-expressing glial progenitor cells: an abundant and widespread population of cycling cells in the adult rat CNS. Mol Cell Neurosci 24:476–488
12. Fernandez-Castaneda A, Gaultier A (2016) Adult oligodendrocyte progenitor cells - multifaceted regulators of the CNS in health and disease. Brain Behav Immun 57:1–7
13. Menn B, Garcia-Verdugo JM, Yaschine C, Gonzalez-Perez O, Rowitch D, Alvarez-Buylla A (2006) Origin of oligodendrocytes in the subventricular zone of the adult brain. J Neurosci 26:7907–7918
14. Gonzalez-Perez O, Alvarez-Buylla A (2011) Oligodendrogenesis in the subventricular zone and the role of epidermal growth factor. Brain Res Rev 67:147–156
15. Tognatta R, Miller RH (2016) Contribution of the oligodendrocyte lineage to CNS repair and neurodegenerative pathologies. Neuropharmacology 110:539–547
16. Miron VE, Boyd A, Zhao JW, Yuen TJ, Ruckh JM, Shadrach JL, van Wijngaarden P, Wagers AJ, Williams A, Franklin RJM et al (2013) M2 microglia and macrophages drive oligodendrocyte differentiation during CNS remyelination. Nat Neurosci 16:1211–1218
17. Lloyd AF, Miron VE (2019) The pro-remyelination properties of microglia in the central nervous system. Nat Rev Neurol 15:447–458
18. Lucchinetti C, Bruck W, Parisi J, Scheithauer B, Rodriguez M, Lassmann H (2000) Heterogeneity of multiple sclerosis lesions: implications for the pathogenesis of demyelination. Ann Neurol 47:707–717
19. Adamo AM, Paez PM, Escobar Cabrera OE, Wolfson M, Franco PG, Pasquini JM, Soto EF (2006) Remyelination after cuprizone-induced demyelination in the rat is stimulated by apotransferrin. Exp Neurol 198:519–529
20. Gomez Pinto LI, Rodriguez D, Adamo AM, Mathieu PA (2018) TGF-beta pro-oligodendrogenic effects on adult SVZ progenitor cultures and its interaction with the Notch signaling pathway. Glia 66:396–412
21. Mathieu PA, Almeira Gubiani MF, Rodriguez D, Gomez Pinto LI, Calcagno ML, Adamo AM (2019) Demyelination-remyelination in the central nervous system: ligand-dependent participation of the notch signaling pathway. Toxicol Sci 171:172–192
22. Dieu RS, Wais V, Sorensen MZ, Marczynska J, Dubik M, Kavan S, Thomassen M, Burton M, Kruse T, Khorooshi R et al (2021) Central nervous system-endogenous TLR7 and TLR9 induce different immune responses and effects on experimental autoimmune encephalomyelitis. Front Neurosci 15:685645

23. Prinz M, Garbe F, Schmidt H, Mildner A, Gutcher I, Wolter K, Piesche M, Schroers R, Weiss E, Kirschning CJ et al (2006) Innate immunity mediated by TLR9 modulates pathogenicity in an animal model of multiple sclerosis. J Clin Invest 116:456–464
24. Marta M (2009) Toll-like receptors in multiple sclerosis mouse experimental models. Ann N Y Acad Sci 1173:458–462
25. Rodriguez JM, Elias F, Flo J, Lopez RA, Zorzopulos J, Montaner AD (2006) Immunostimulatory PyNTTTTGT oligodeoxynucleotides: structural properties and refinement of the active motif. Oligonucleotides 16:275–285
26. Elias F, Flo J, Lopez RA, Zorzopulos J, Montaner A, Rodriguez JM (2003) Strong cytosine-guanosine-independent immunostimulation in humans and other primates by synthetic oligodeoxynucleotides with PyNTTTTGT motifs. J Immunol 171:3697–3704
27. Hernando Insua A, Montaner AD, Rodriguez JM, Elias F, Flo J, Lopez RA, Zorzopulos J, Hofer EL, Chasseing NA (2007) IMT504, the prototype of the immunostimulatory oligonucleotides of the PyNTTTTGT class, increases the number of progenitors of mesenchymal stem cells both in vitro and in vivo: potential use in tissue repair therapy. Stem Cells 25:1047–1054
28. Rodriguez JM, Elias F, Montaner A, Flo J, Lopez RA, Zorzopulos J, Franco RJ, Lenial SP, Lopez Salon M, Pirpignani ML et al (2006) Oligonucleotide IMT504 induces an immunogenic phenotype and apoptosis in chronic lymphocytic leukemia cells. Medicina 66:9–16
29. Coronel MF, Hernando-Insua A, Rodriguez JM, Elias F, Chasseing NA, Montaner AD, Villar MJ (2008) Oligonucleotide IMT504 reduces neuropathic pain after peripheral nerve injury. Neurosci Lett 444:69–73
30. Leiguarda C, Coronel MF, Montaner AD, Villar MJ, Brumovsky PR (2018) Long-lasting ameliorating effects of the oligodeoxynucleotide IMT504 on mechanical allodynia and hindpaw edema in rats with chronic hindpaw inflammation. Neurosci Lett 666:17–23
31. Leiguarda C, Potilinski C, Rubione J, Tate P, Villar MJ, Montaner A, Bisagno V, Constandil L, Brumovsky PR (2021) IMT504 provides analgesia by modulating cell infiltrate and inflammatory milieu in a chronic pain model. J Neuroimmune Pharmacol 16:651–666
32. Chahin A, Opal SM, Zorzopulos J, Jobes DV, Migdady Y, Yamamoto M, Parejo N, Palardy JE, Horn DL (2015) The novel immunotherapeutic oligodeoxynucleotide IMT504 protects neutropenic animals from fatal Pseudomonas aeruginosa bacteremia and sepsis. Antimicrob Agents Chemother 59:1225–1229
33. Hernando-Insua A, Rodriguez JM, Elias F, Flo J, Lopez R, Franco R, Lago N, Zorzopulos J, Montaner AD (2010) A high dose of IMT504, the PyNTTTTGT prototype immunostimulatory oligonucleotide, does not alter embryonic development in rats. Oligonucleotides 20:33–36
34. Franco R, Rodriguez JM, Elias F, Hernando-Insua A, Flo J, Lopez R, Nagle C, Lago N, Zorzopulos J, Horn DL et al (2014) Non-clinical safety studies of IMT504, a unique non-CpG oligonucleotide. Nucleic acid therapeutics 24:267–282
35. Zeis T, Enz L, Schaeren-Wiemers N (2016) The immunomodulatory oligodendrocyte. Brain Res 1641:139–148
36. Zelek WM, Watkins LM, Howell OW, Evans R, Loveless S, Robertson NP, Beenes M, Willems L, Brandwijk R, Morgan BP (2019) Measurement of soluble CD59 in CSF in demyelinating disease: evidence for an intrathecal source of soluble CD59. Mult Scler 25:523–531
37. Aparicio E, Mathieu P, Pereira Luppi M, Almeira Gubiani MF, Adamo AM (2013) The Notch signaling pathway: its role in focal CNS demyelination and apotransferrin-induced remyelination. J Neurochem 127:819–836
38. Franco PG, Silvestroff L, Soto EF, Pasquini JM (2008) Thyroid hormones promote differentiation of oligodendrocyte progenitor cells and improve remyelination after cuprizone-induced demyelination. Exp Neurol 212:458–467
39. Rosato Siri MV, Badaracco ME, Pasquini JM (2013) Glatiramer promotes oligodendroglial cell maturation in a cuprizone-induced demyelination model. Neurochem Int 63:10–24
40. Dawes CJ (1988) Introduction to biological electron microscopy: theory and techniques. Publisher Burlington, VT: Ladd Research Industries, Inc
41. Mercer EH, Birbeck MSC (1972) Electron microscopy. A handbook for biologists, third edn. Blackwell Scientific Publications
42. Oberhammer F, Fritsch G, Schmied M, Pavelka M, Printz D, Purchio T, Lassmann H, Schulte-Hermann R (1993) Condensation of the chromatin at the membrane of an apoptotic nucleus is not associated with activation of an endonuclease. J Cell Sci 104(Pt 2):317–326
43. McCarthy KD, de Vellis J (1980) Preparation of separate astroglial and oligodendroglial cell cultures from rat cerebral tissue. J Cell Biol 85:890–902
44. Leiguarda C, Villarreal A, Potilinski C, Pelissier T, Coronel MF, Bayo J, Ramos AJ, Montaner A, Villar MJ, Constandil L et al (2021) Intrathecal administration of an anti-nociceptive non-CpG oligodeoxynucleotide reduces glial activation and central sensitization. J Neuroimmune Pharmacol 16:818–834
45. Di Rienzo JA, Guzmán AW, Casanoves F (2002) Comparisons method based on the distribution of the root node distance of a binary tree. J Agric Biol Environ Stat 7:1–14
46. Pinheiro JC, Bates DM (2004) Mixed-effects models in S and S-Plus. Springer, U.S.A, p. 206
47. Coetzee T, Fujita N, Dupree J, Shi R, Blight A, Suzuki K, Suzuki K, Popko B (1996) Myelination in the absence of galactocerebroside and sulfatide: normal structure with abnormal function and regional instability. Cell 86:209–219
48. Chomiak T, Hu B (2009) What is the optimal value of the g-ratio for myelinated fibers in the rat CNS? A theoretical approach. PLoS one 4:e7754
49. Dendrou CA, Fugger L, Friese MA (2015) Immunopathology of multiple sclerosis. Nat Rev Immunol 15:545–558
50. Krieg AM, Yi AK, Matson S, Waldschmidt TJ, Bishop GA, Teasdale R, Koretzky GA, Klinman DM (1995) CpG motifs in bacterial DNA trigger direct B-cell activation. Nature 374:546–549
51. Zorzopulos J, Opal SM, Hernando-Insua A, Rodriguez JM, Elias F, Flo J, Lopez RA, Chasseing NA, Lux-Lantos VA, Coronel MF et al (2017) Immunomodulatory oligonucleotide IMT504: effects on mesenchymal stem cells as a first-in-class immunoprotective/immunoregenerative therapy. World J Stem Cells 9:45–67
52. Marta M, Andersson A, Isaksson M, Kampe O, Lobell A (2008) Unexpected regulatory roles of TLR4 and TLR9 in experimental autoimmune encephalomyelitis. Eur J Immunol 38:565–575
53. McMurran CE, Zhao C, Franklin RJM (2019) Toxin-based models to investigate demyelination and remyelination. Methods Mol Biol 1936:377–396
54. Matsushima GK, Morell P (2001) The neurotoxicant, cuprizone, as a model to study demyelination and remyelination in the central nervous system. Brain Pathol 11:107–116
55. Frakes AE, Ferraiuolo L, Haidet-Phillips AM, Schmelzer L, Braun L, Miranda CJ, Ladner KJ, Bevan AK, Foust KD, Godbout JP et al (2014) Microglia induce motor neuron death via the classical NF-kappaB pathway in amyotrophic lateral sclerosis. Neuron 81:1009–1023
56. Miron VE (2017) Microglia-driven regulation of oligodendrocyte lineage cells, myelination, and remyelination. J Leukoc Biol 101:1103–1108
57. Domingues HS, Portugal CC, Socodato R, Relvas JB (2016) Oligodendrocyte, astrocyte, and microglia crosstalk in myelin development, damage, and repair. Front Cell Dev Biol 4:71
58. Domingues HS, Cruz A, Chan JR, Relvas JB, Rubinstein B, Pinto IM (2018) Mechanical plasticity during oligodendrocyte differentiation and myelination. Glia 66:5–14

59. Santos EN, Fields RD (2021) Regulation of myelination by microglia. Sci Adv 7:eabk1131
60. Shigemoto-Mogami Y, Hoshikawa K, Goldman JE, Sekino Y, Sato K (2014) Microglia enhance neurogenesis and oligodendrogenesis in the early postnatal subventricular zone. J Neurosci 34:2231–2243
61. Rodriguez JM, Marchicio J, Lopez M, Ziblat A, Elias F, Flo J, Lopez RA, Horn D, Zorzopulos J, Montaner AD (2015) PyNTTT TGT and CpG immunostimulatory oligonucleotides: effect on granulocyte/monocyte colony-stimulating factor (GM-CSF) secretion by human CD56+ (NK and NKT) cells. PloS One 10:e0117484
62. Smets I, Fiddes B, Garcia-Perez JE, He D, Mallants K, Liao W, Dooley J, Wang G, Humblet-Baron S, Dubois B et al (2018) Multiple sclerosis risk variants alter expression of co-stimulatory genes in B cells. Brain 141:786–796
63. Patel J, Pires A, Derman A, Fatterpekar G, Charlson RE, Oh C, Kister I (2022) Development and validation of a simple and practical method for differentiating MS from other neuroinflammatory disorders based on lesion distribution on brain MRI. J Clin Neurosci 101:32–36